Pre-Clinical Research Report

Journal of INTERNATIONAL MEDICAL RESEARCH

Journal of International Medical Research
48(2) 1–13

DOI: 10.1177/0300060519897185
journals.sagepub.com/home/imr
SAGE

Heparin coated meta-organic framework co-delivering doxorubicin and quercetin for effective chemotherapy of lung carcinoma

Xiaojun Sun, Yongxing Li, Liang Xu, Xinyu Shi, Mengmin Xu, Xuefang Tao and Guobiao Yang

Abstract

Objective: To develop and evaluate a drug delivery system (DDS) capable of targeting cancer cells while at the same time delivering two chemotherapeutic agents to overcome multidrug resistance (MDR).

Methods: This study developed a DDS composed of heparin (HA)-coated meta-organic framework (MOF) nanoparticles (HM) designed to deliver doxorubicin (Dox) and quercetin (Que). A range of *in vitro* and *in vivo* studies were conducted to determine the characteristics of the HM/Dox/Que nanoparticles, their ability to produce cytotoxic effects in Dox-resistant A549/Dox cells and target and treat solid tumours in a mouse xenograft model of human lung carcinoma.

Results: This study demonstrated that the HM/Dox/Que nanoparticles reduced cell viability, increased apoptosis, arrested cells in the G0/G1 phase of the cell cycle and reversed MDR in A549/Dox cells *in vitro* when compared with mono-drug delivery. In a mouse xenograft model of human lung carcinoma, the HM/Dox/Que nanoparticles targeted the tumours and reduced tumour growth as determined by tumour volume.

Conclusion: The use of HM/Dox/Que nanoparticles might be a viable alternative to traditional chemotherapy of lung carcinoma.

Keywords

Heparin, meta-organic framework, doxorubicin, quercetin, chemotherapy, lung carcinoma

Date received: 29 August 2019; accepted: 3 December 2019

Department of Respiratory Medicine, Affiliated Hospital of Shaoxing University of Arts and Sciences, Shaoxing, Zhejiang Province, China

Corresponding author:
Guobiao Yang, Department of Respiratory Medicine, Affiliated Hospital of Shaoxing University of Arts and Sciences, 999 South Zhongxing Road, Yuecheng District, Shaoxing 312000, Zhejiang Province, China.
Email: yanggb11@yeah.net

Introduction

To date, cancer chemotherapy usually fails to meet the desired anticancer performance due to the development of multidrug resistance (MDR) in many cancer types.[1–3] To this end, the combined administration of different types of anticancer drugs has gradually emerged and provides a more effective cancer chemotherapy.[4,5] Previous studies have demonstrated that combination chemotherapy can greatly enhance cytotoxicity while reducing the dosage, which significantly reduces the unwanted side-effects of anticancer drugs.[5] The basic principle for combination chemotherapy is co-deliver at least two drugs targeting different biological pathways, which ensures high cytotoxicity to the cancer cells.[6,7] However, combination therapy is greatly dependent upon the assistance of drug delivery systems (DDS) to precisely control the dosage, proportion and even the sequence of delivery of the loaded cargos. Considering that most of the currently adopted DDSs are not able to satisfy the first two basic requirements, the introduction of a well-designed DDS is the prerequisite for effective combination therapy.[2]

Over the past few decades, the development of a novel DDS that is suitable for cancer chemotherapy has been the focus of considerable pharmaceutical research. Various DDSs based on different materials have been developed to test their feasibility in cancer therapy.[8–10] In particular, the outstanding merits of meta-organic framework (MOF) nanoparticles, including high biocompatibility, low cost and decent drug loading of different drugs (from hydrophilic to hydrophobic), have made it suitable for the chemotherapy of cancer.[11,12] Apart from the carriers, the tumour homing capability of the resulting DDS is another important issue that should be taken into consideration.[13] In recent years, heparin (HA), which offers the combination of shielding and targeting, has become the most widely studied material. For example, HA-modified DDSs were found to home to CD44 receptor overexpressing cancer cells with high efficiency while at the same time significantly alleviating liver capture.[14] Previous studies have provided evidence that positive targeting is better than passive targeting, which will be the future direction of DDS design.[15,16]

Doxorubicin (Dox) is one of the most commonly used drugs for the chemotherapy of various cancers.[1] However, the severe side-effects of Dox remain a major concern that hampers its performance in many clinical trials.[3] As a result, combination therapy is believed to be an ideal approach in order to minimize the MDR of tumour cells and reduce the Dox-related side-effects.[17,18]

Quercetin (Que) is one of the most abundant triterpenoids in plants, which is known for its ability to regulate many pharmacological processes and for having antitumor activity.[19]It has been demonstrated that the anticancer activity of Que is facilitated via the activation of the adenosine monophosphate (AMP)-activated protein kinase (AMPK) pathway, suppression of the phosphoinositide 3-kinase/ (PI3K)/AKT/ mammalian target of rapamycin/nuclear factor-κB pathway, upregulation p53 activation and the apoptosis pathway.[20] In recent studies, Que has been reported to achieve improved outcomes with enhanced apoptosis and reduced side-effects when applied with other chemotherapy reagents.[21,22] Although the combination of both drugs for cancer therapy has been reported by some previous articles,[3,20] there is still more work to be done. For example, the *in vivo* performance of both drugs in lung cancer has not been explored,[23] their ability to reverse MDR has not been demonstrated[24] and experiments have not been extended using lung cancer cell lines.[25]

This current study selected the combination of Dox and Que due to their distinct

mechanisms of action. The hybrid nanoparticle HA-coated MOF (HM) was employed to load both drugs onto the same delivery system in order to construct a DDS for the chemotherapy of lung carcinoma.

Materials and methods

Reagents

All chemical reagents were of analytical grade and purchased from Sigma-Aldrich (St Louis, MO, USA).

Preparation of the DDS nanoparticles

First, $Zn(NO_3)_2{\cdot}_6H_2O$ (10 mg), Dox (5 mg) and Que (5 mg) were dissolved 10 ml of ethanol. Then, 2-methylimidazole (12 mg) was quickly added to the ethanol solution and the mixture was vigorously stirred for 30 s. The mixture was centrifuged in a Sigma 3-30KS centrifuge (Sigma-Aldrich) at 8000 ***g*** for 10 min at room temperature to obtain the dual-loaded core (MOF/Dox/Que).

In order to add the coating of HA to the MOF to construct the HA/Dox/Que nanoparticles, an aqueous solution of MOF (1 mg/ml) was mixed with different ratios of HA using a vortexer. After being sonicated for 30 min (100 W), the HM/Dox/Que was obtained by centrifuging the mixture in a Sigma 3-30KS centrifuge (Sigma-Aldrich) at 10 000 ***g*** for 10 min at room temperature.

Mono-drug delivery systems (HM/Dox and HM/Que) were prepared by adding only one drug during the drug loading process, while the method of coating of HA to the MOF was the same as that for the dual-loaded core HM/Dox/Que.

Analysis of the DDS nanoparticles

The morphology and particle size of different nanoparticles were observed by transmission electron microscopy (JEM-1200; JEOL, Tokyo, Japan) at an accelerating voltage of 80 kV. Moreover, the particle size distribution and zeta potential were further determined using a Zeta/Particle Analyzer (Litesizer 500; Anton Paar, Graz, Austria).

The freshly prepared HM/Dox/Que was diluted with 0.01 M phosphate buffered saline (PBS; pH 7.4; 1:10, v/v) or mouse plasma (from study mice). Afterwards, the change in particle size was monitored for 48 h to estimate the colloidal stability.

For the haemolysis assay, red blood cells (RBCs) obtained from mice were diluted in saline to obtain a 2% suspension. The HM/Dox/Que was added to the RBC suspension to achieve the designated concentrations and the mixture was incubated at 37°C for 1 h. After that, samples were centrifuged at 3500 ***g*** at room temperature for 10 min using a high-speed refrigerated centrifuge (Model 7780; KUBOTA, Tokyo, Japan) and the supernatants were analysed using a Multiskan Sky Microplate Spectrophotometer at 545 nm according to the manufacturer's instructions (ThermoFisher Scientific, Waltham, MA, USA). The RBC suspension was incubated with distilled water and saline under the same conditions to form the positive (100% haemolysis) and negative (0% haemolysis) controls, respectively.

The HM/Dox/Que (containing 100 μg DOX/Que) was loaded into a dialysis bag (MWCO: 7000 Da) and immersed in a plastic tube charged with 0.01 M PBS (25 ml) at pH 7.4 or pH 5.5. The plastic tubes were fixed in a thermostatic shaker (HZQ-C; Harbin Dongming Medical Instrument Factory, Harbin, China) at 37°C with a stirring speed of 100 rpm. At predetermined time-points, the primary medium was replaced by an equal volume of fresh medium and the drug concentration within the primary medium was determined. The Dox content was determined using a fluorescence spectrophotometer (F-2700; Hitachi, Tokyo, Japan; excitation wavelength: 505 nm; emission wavelength: 605 nm).

The concentration of Que was measured using high-performance liquid chromatography (LC-2030; Shimadzu, Tokyo, Japan) with the following conditions: Agilent SB-C18 880975-902 column (4.6 mm, 250 mm, 5 μm); mobile phase was 0.1% trifluoroacetic acid aqueous solution: acetonitrile/methanol mixture (17:1) = 1:9 (v/v). The temperature was 30°C, the flow rate was 1 ml/min and the detection wavelength was 210 nm.

In vitro anticancer assay

Dox-resistant human lung carcinoma A549/Dox cells were purchased from the American Type Culture Collection (ATCC, Manassas, VA, USA) and cultured in Dulbecco's modified Eagle's medium supplemented with 10% fetal bovine serum (both from Gibco, Carlsbad, CA, USA) at 37°C in a humidified atmosphere containing 5% carbon dioxide. Cells were treated with different formulations at different drug concentrations (HM/Dox, HM/Que and HM/Dox/Que at the drug concentrations of 0.1, 0.5, 1, 2, 5 and 10 μg/ml) for 48 h after which their rate of cell viability was measured using a 3-(4,5-Dimethylthiazol-2-yl)-2,5- diphenyltetrazolium bromide, a tetrazole (MTT) assay kit (Solarbio, Beijing, China). To determine their synergistic effect, the combination index (CI) was calculated using the following formula: $CI = Dose1/Dosex1 + Dose2/Dosex2$, where Dose1 and Dose2 are the concentrations of drug 1 and drug 2 inhibiting x% cells; and Dosex1 and Dosex2 are the concentrations of drug 1 and drug 2 alone inhibiting x% cells. A multicellular tumour sphere (MCTS) model was subjected to treatment with different formulations (HM/Dox, HM/Que and HM/Dox/Que at the drug concentration of 2 μg/ml) for 4 days. The MCTSs were developed using the following protocol. In brief, a 96-well tissue culture plate was covered with an autoclaved agarose solution (1.5% w/v; 50 μl/well) and then cooled to room temperature. A549/Dox cells were seeded at a density of 2×10^3 cells per well and incubated for 4 days to grow into MCTSs.

Apoptosis and cell cycle analyses

A549/Dox cells were seeded into a 6-well tissue culture plate at a cell concentration of 2×10^5 cells per well and allowed to grow overnight. Afterwards, cells were treated with HM/Dox, HM/Que and HM/Dox/Que at the drug concentration of 5 μg/ml for 24 h. Then cells were treated with an apoptosis kit (Solarbio) according to the manufacturer's instructions and then subjected to fluorometric analysis using flow cytometry (NovoCyte Flow Cytometer; ACEA Biosciences, Beijing, China) to analyse the positive apoptotic cells. For the cell cycle analysis, cells were cultured as described above and treated with HM/Dox, HM/Que and HM/Dox/Que at the drug concentration of 5 μg/ml for 48 h or 72 h. The cells were then treated with a cell cycle kit (Solarbio) according to the manufacturer's instructions and then subjected to fluorometric analysis using flow cytometry to analyse the distribution of cells in the different phases of the cell cycle.

Western blot analyses

Total protein was extracted from 1×10^6 A549/Dox cells using ice-cold RIPA Lysis and Extraction Buffer (ThermoFisher Scientific) and quantified using a Pierce BCA protein assay reagent kit (Pierce Biotechnology, Rockford, IL, USA). The proteins (50 mg per lane) were separated by 10% sodium dodecyl sulphate–polyacrylamide gel electrophoresis at 150 V for 90 min. The proteins were then transferred to polyvinylidene fluoride membranes (Millipore, Billerica, MA, USA) using

electroblot apparatus at 80 V for 1 h (Bio-Rad, Hercules, CA, USA). The membranes were incubated in blocking solution consisting of Tris-buffered saline-Tween 20 (TBST; pH 7.5; 20 mmol/l Tris–HCl, 150 mmol/l sodium chloride, 0.1% Tween-20) containing 5% nonfat milk at room temperature for 1 h. The membranes were then incubated with rabbit antihuman antibodies for cysteinyl aspartate specific proteinase 3 (Caspase 3), cytochrome C (Cyt C), B-cell lymphoma-2 (Bcl-2), P- glycoprotein (P-gp) or glyceraldehyde-3-phosphate dehydrogenase (GAPDH) at the dilution of 1:1000 (Cell Signaling Technology, Danvers, MA, USA) at 4°C overnight. The membranes were then washed with TBST (pH 7.5) three times and incubated with horseradish peroxidase-conjugated goat antirabbit secondary antibody (dilution 1:4000, Cell Signaling Technology) for 1 h at room temperature. The membranes were developed using an enhanced chemiluminescence reagent kit (Pierce Biotechnology) and exposed to X-radiography film. Immunoblots were scanned using a densitometer (AC186; Bio-Rad).

Analysis of intracellular drug concentrations

A549/Dox cells were seeded into 6-well tissue culture plates at a density of 3×10^5 cells per well and cultured overnight in order to achieve 80–90% confluence. After that, the primary culture medium was removed and replaced with an equal volume of serum-free medium containing free HM/Dox and HM/Dox/Que (DOX concentration: 2 μg/ml). At predetermined time intervals (4, 8 and 12 h), cells were trypsinized, collected and dispersed in 5 ml of DOX extracting solution (ethanol: 0.6 M HCl, 1:1, v/v), followed by ultrasonication at 400 W in an ice bath for 40 times. The mixture was incubated at 4°C for 24 h, followed by centrifugation at 15000 ***g*** (4°C) for 10 min using a high-speed refrigerated centrifuge (Model 7780; KUBOTA). The supernatant was collected and subjected to fluorescence measurement as described above.

Tumour targeting assay

Coumarin-6 was encapsulated into HA and used to construct the DDS. Briefly, 5×10^5 A549/Dox cells were pretreated with HA (100 μg/ml) or 0.01 M PBS (pH 7.4) for 2 h, followed by incubation with different formulations for different time intervals (free C6, MOF/C6 or HM/C6 at the C6 concentration of 1 μg/ml for 2, 4 and 6 h). At each time interval, cells were collected and subjected to flow cytometric analysis of mean fluorescence intensity of C6 in cells.

To study the *in vivo* tumour targeting of DDS, indocyanine green (ICG) was loaded to form ICG-labelled DDS and injected into A549/Dox tumour-bearing mice through the tail vein (see below for details). At 24 h post-administration, the mice were sacrificed, their organs and tumour tissues were collected and subjected to fluorometric analysis (Bio-Real; Geneway, Vienna, Austria).

In vivo anticancer efficacy

Male BALB/c nude mice (30 mice, aged 5 weeks, 22 g; Slack Laboratory Animals, Shanghai, China) were housed in specific pathogen-free conditions with free access to food and water, in a 13-h light/11-h dark cycle. The study was carried out in strict accordance with the National Institutes of Health Guidelines for the Care and Use of Laboratory Animals. The study was also reviewed and approved by the Institutional Animal Care and Use Committee of Shaoxing University of Arts and Sciences, Zhejiang Province, China (no. 201809231).

Briefly, suspensions of A549/Dox (2×10^6) cells in 100 μl of 0.01 M PBS

(pH 7.4) were inoculated subcutaneously in the flanks of mice. Tumour sizes were measured using a Vernier calliper and tumour volumes were calculated as $V = a^2 \times b/2\,mm^3$ (a: minor axis; b: major axis).

Tumour-bearing mice were selected and randomly assigned to five groups ($n = 6$). The mice were treated with different formulations at the Dox dosage of 7.5 mg/kg and Que dosage of 20 mg/kg. The measurement of tumour volume and body weight was repeated seven times before drug administration once every 2 days.

Statistical analyses

All statistical analyses were performed using the SPSS® statistical package, version 11.0 (SPSS Inc., Chicago, IL, USA) for Windows®. Data are presented as mean ± SD and were compared using factorial analysis of variance or Student's *t*-test, as appropriate. A *P*-value <0.05 was considered to be statistically significant.

Results

As shown in Figure 1a, the size distribution of the HM/Dox/Que nanoparticles was uniformly distributed at around 100 nm with a small polydispersion index of 0.042 and a zeta potential of –28.23 mV (Figure 1b).

As shown in Figure 2a, the change in the size of the HM/Dox/Que nanoparticles was not significant over time up to 48 h when incubated with mouse plasma or 0.01 M PBS (pH 7.4). The haemolysis assay shown in Figure 2b demonstrated that the HM/Dox/Que nanoparticles caused almost no haemolysis of red blood cells.

The drug release profiles of HM/Dox/Que are presented in Figure 3. Under physiological conditions (pH 7.4), both Dox and Que were released slowly from the DDS nanoparticles. In contrast, under pathological conditions (pH 5.5), the drug release was elevated.

The *in vitro* anticancer effects of HM/Dox/Que in human lung carcinoma A549/Dox cells were studied using an MTT assay. As shown in Figure 4a, the lowest CI of 0.23 was achieved when the w/w ratio of Dox/Que was 1/1, which indicated that the combination effect of the two drugs was optimal at this ratio. An MTT assay using this optimal drug ratio was

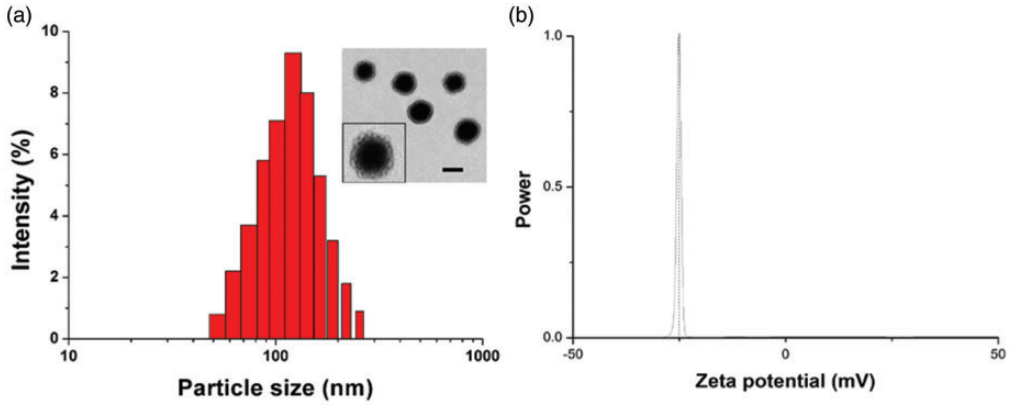

Figure 1. Analysis of the drug delivery system nanoparticles. The size distribution of the heparin-coated meta-organic framework/doxorubicin/quercetin (HM/Dox/Que) nanoparticle drug delivery system. Inserted image shows a transmission electron micrograph of the HM/Dox/Que nanoparticles. Scale bar: 100 nm (a). The zeta potential of the HM/Dox/Que nanoparticles was −28.23 mV (b).

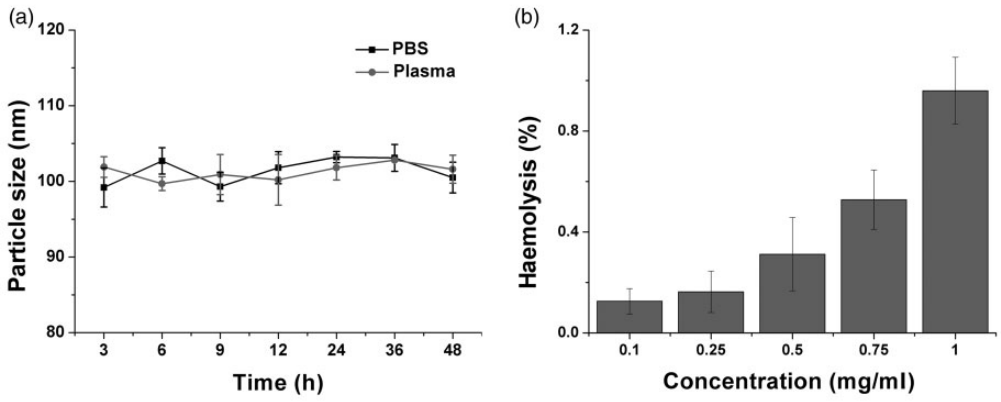

Figure 2. (a) Time-dependent changes (3–48 h) in the size of the heparin-coated meta-organic framework/doxorubicin/quercetin (HM/Dox/Que) nanoparticles in 0.01 M phosphate-buffered saline (PBS; pH 7.4) and mouse plasma. (b) The concentration-dependent haemolysis of a 2% red blood cell suspension caused by HM/Dox/Que nanoparticles. Experiments were undertaken three times and the data expressed as mean ± SD.

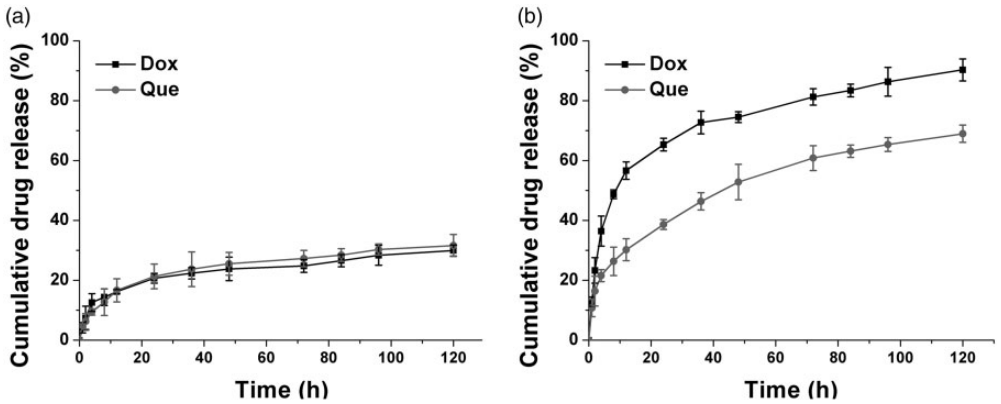

Figure 3. The drug release of doxorubicin (Dox) and quercetin (Que) from the heparin-coated meta-organic framework/doxorubicin/quercetin (HM/Dox/Que) nanoparticles at pH 7.4 (a) and pH 5.5 (b). Experiments were undertaken three times and the data expressed as mean ± SD.

undertaken in A549/Dox cells. As illustrated in Figure 4b, compared with the mono-drug delivery systems, the combination of Dox and Que greatly reduced the dosage to achieve the same cytotoxicity. The IC_{50} was achieved at the dosage of 2 μg/ml at 48 h post-incubation. The results in the MCTS model demonstrated similar findings (Figure 4c).

The effect on A549/Dox cell apoptosis following treatment with different formulations was investigated. As demonstrated in Figure 5a, compared with the mono-drug delivery systems, the rate of apoptosis in the HM/Dox/Que group was significantly elevated to 84.7% ($P < 0.01$). As shown in Figure 5b, the combination therapy of HM/Dox/Que increased G0/G1 phase

(a)

w/w ratio (Dox/Que)	CI
1/10	0.56
1/5	0.69
1/2	0.26
1/1	0.23
2/1	0.31
5/1	0.46
10/1	0.52

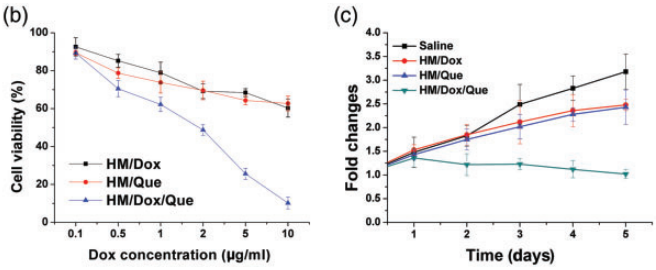

Figure 4. (a) The combination index (CI) of the heparin-coated meta-organic framework/doxorubicin/quercetin (HM/Dox/Que) nanoparticle drug delivery system in A549/Dox cells treated for 48 h at different Dox/Que ratios (w/w). (b) The cell viability was measured using an 3-(4,5-Dimethylthiazol-2-yl)-2,5-diphenyltetrazolium bromide, a tetrazole (MTT) assay kit after the A549/Dox cells had been treated with HM/Dox, HM/Que and HM/Dox/Que (Dox/Que = 1, w/w) at different drug concentrations for 48 h. (c) The volume variations of multicellular tumour sphere model treated with different formulations. Experiments were undertaken three times and the data expressed as mean ± SD.

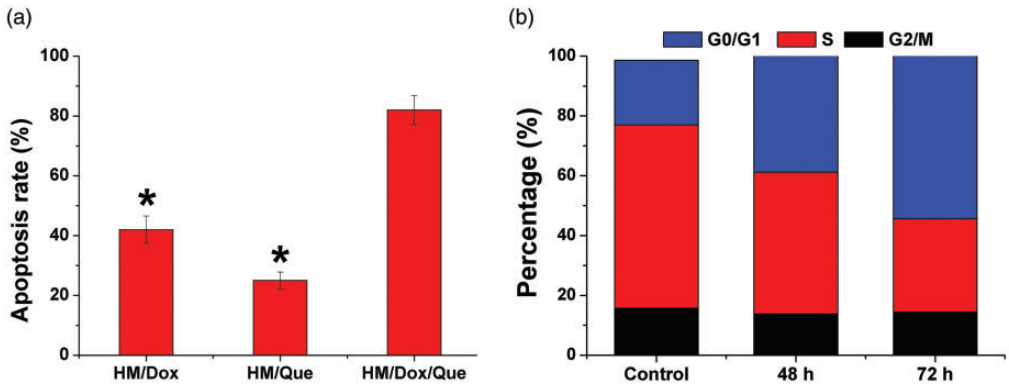

Figure 5. (a) The rate of apoptosis of A549/Dox cells treated with different formulations of the heparin-coated meta-organic framework/doxorubicin/quercetin (HM/Dox/Que) nanoparticle drug delivery system at the drug concentration of 2 μg/ml for 48 h (Dox/Que = 1, w/w). (b) The cell cycle variations of A549/Dox cells treated with HM/Dox/Que for different time intervals. Experiments were undertaken three times and the data expressed as mean ± SD. *$P < 0.01$ versus HM/Dox/Que; Student's *t*-test.

arrest and reduced the percentage of cells in S phase.

Moreover, the ability to reverse MDR in A549/Dox cells was further investigated by measuring the intracellular time-dependent drug accumulation of Dox. As shown in Figure 6a, compared with the mono-drug delivery system, the co-delivery of Dox and Que resulted in enhanced drug accumulation within cells, which was positively dependent up incubation duration. The variations of cellular protein levels were measured using Western blot analysis to investigate the possible reasons for the reversal of MDR. As shown in Figure 6b, the mono delivery of Dox was able to trigger P-gp overexpression in A549/Dox cells. Most importantly, the treatment of Que-containing formulations reduced the expression of P-gp protein in A549/Dox cells as compared with Que-deficient formulations, which was comparable with the downregulation of P-gp levels.

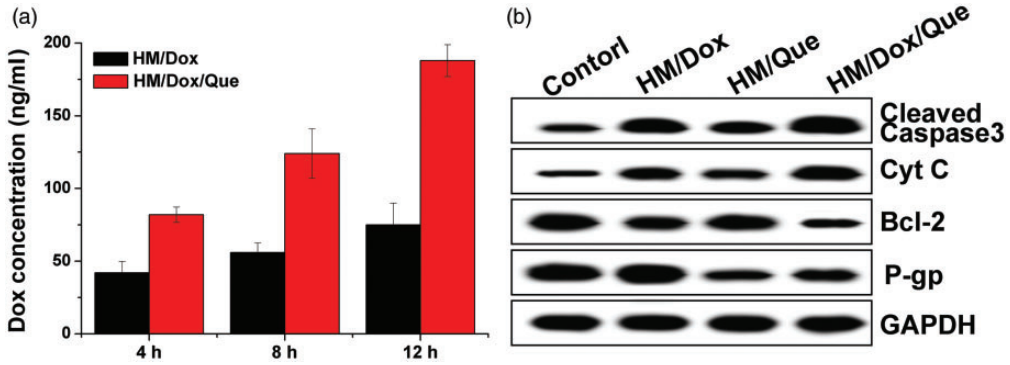

Figure 6. (a) The intracellular drug concentration within A549/Dox cells treated with different formulations of the heparin-coated meta-organic framework/doxorubicin/quercetin (HM/Dox/Que) nanoparticle drug delivery system for different time intervals. Experiments were undertaken three times and the data expressed as mean ± SD. (b) Western blot analysis of protein variations after A549/Dox cells had been treated with different HM/Dox/Que nanoparticle formulations for 48 h. Experiments were undertaken three times and the data expressed as mean ± SD. Caspase 3, cysteinyl aspartate specific proteinase 3; Cyt C, cytochrome C; Bcl-2, B-cell lymphoma-2; P-gp, P-glycoprotein; GAPDH, glyceraldehyde-3-phosphate dehydrogenase.

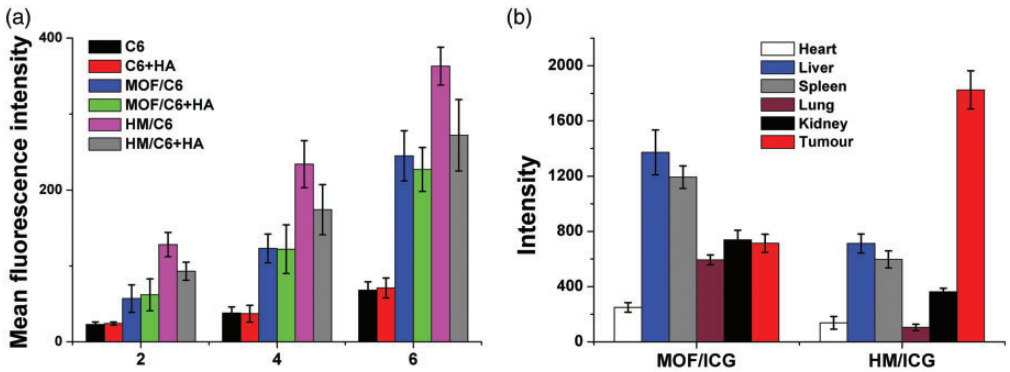

Figure 7. The *in vitro* and *in vivo* targeting assays of the heparin-coated meta-organic framework/doxorubicin/quercetin (HM/Dox/Que) nanoparticle drug delivery system. Intracellular uptake of various formulations in A549/Dox cells after incubation for 2, 4 and 6 h (a). To study the *in vivo* tumour targeting of the drug delivery system (DDS), indocyanine green (ICG) was loaded to form ICG-labelled DDS and injected into A549/Dox tumour-bearing mice through the tail vein. At 24 h post-administration, the mice were sacrificed, their organs and tumour tissues were collected and subjected to fluorometric analysis of C6 levels (b). Experiments were undertaken three times and the data expressed as mean ± SD. C6, coumarin-6; HA, heparin; MOF, meta-organic framework; HM, heparin-coated meta-organic framework.

As demonstrated in Figure 7a, the *in vitro* intracellular uptake of all formulations was positively associated with incubation duration in A549/Dox cells. However, free C6 and C6 + HA showed relatively slow accumulation in A549/Dox cells. Cells treated with nanoparticles showed elevated C6 signal inside the cells. Moreover, it was noted that the fluorescence intensity in the HM-treated group (HM/C6) was 1.79-fold

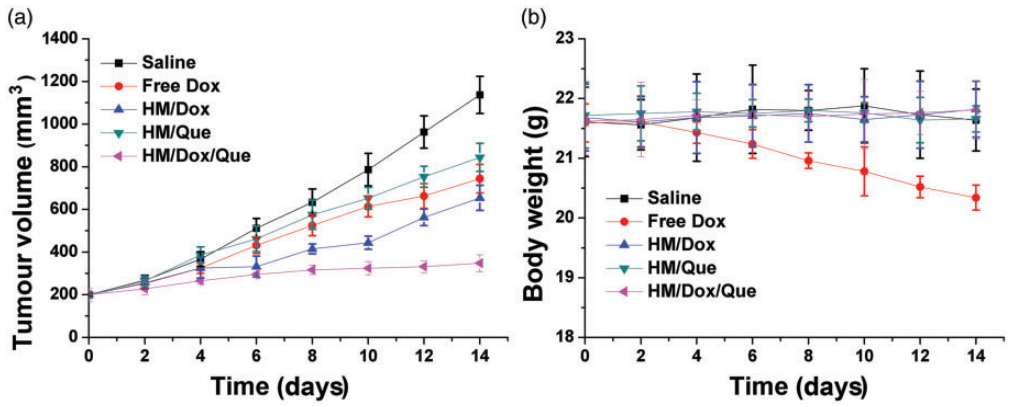

Figure 8. The tumour volume (a) and body weight (b) variations of A549/Dox tumour-bearing mice treated with different formulations of the heparin-coated meta-organic framework/doxorubicin/quercetin (HM/Dox/Que) nanoparticle drug delivery system. Data expressed as mean ± SD.

higher than that of the MOF-treated (MOF/C6) group after incubation for 6 h. After exposure to an excess of HA for 2 h, the intracellular C6 signals in different groups were recorded and compared. As expected, the intracellular uptake of HM/C6 was reduced in A549/Dox cells after HA pretreatment, while minimal changes were observed in MOF-treated A549/Dox cells pretreated with HA.

As shown in Figure 7b, MOF and HM were labelled with ICG and then injected intravenously into A549/Dox tumour-bearing mice. At 24 h post nanoparticle administration, the mice were sacrificed to harvest the organs and tumours to determine the fluorescence signals using *ex vivo* imaging. In line with results in Figure 8a, the HM/ICG showed a 2.54-fold increase of the fluorescence signal in tumours compared with the MOF/ICG group.

The *in vivo* antitumor efficacy of the DDS nanoparticles was assessed using A549/Dox tumour-bearing mice. As shown in Figure 8a, in line with the *in vitro* MTT assay, the anticancer effect of HM/Dox was much better than that of free Dox. The *in vivo* experiments further confirmed that the co-delivery of Dox and Que was superior to the mono-drug delivery systems in terms of reducing tumour volume. In addition, the variations of body weight shown in Figure 8b suggested that free Dox without the aid of DDS was not suitable because it reduced body weight. In contrast, the HM/Dox/Que nanoparticles showed almost no adverse effects on body weight in mice.

Discussion

This current study investigated a hybrid nanoparticle that was employed to load two drugs, Dox and Que, onto the same DDS for the chemotherapy of lung carcinoma *in vitro* and *in vivo*. The current results demonstrated the stability of the HM/Dox/Que nanoparticle under physiological conditions. The negligible haemolysis caused by HM/Dox/Que suggested that it was highly biocompatible in terms of it being a DDS.[26] The increased drug release that was observed at pH 5.5 might have been due to the pH-responsive decomposition of MOF. It would be beneficial for HM/Dox/Que to responsively release the loaded drugs in tumour tissues instead of in the physiological environment. The MTT assay

demonstrated that compared with the mono-drug delivery systems, the combination of both drugs reduced the IC_{50} to a much lower level. These findings demonstrated that Dox and Que achieved a synergistic effect on inhibiting cell growth. The apoptosis and cell cycle assays also supported the results of the MTT assay, which were comparable with a previous report.[27] These current results strongly suggested that the combination of both drugs was capable of increasing the rate of apoptosis of A549/Dox cells via cell cycle arrest at the G0/G1 phase and a reduction in the percentage of cells in the S phase.

The time-dependent cellular drug retention assay in the current study demonstrated that the integration of Que into the DDS could reverse the MDR in A549/Dox cells, which was beneficial for the accumulation of Dox in cells for a better performance. The Western blot assay in the current study also revealed that Que could effectively reverse the MDR induced by Dox through the downregulation of P-gp expression, which was in line with previous reports that chemotherapy was responsible for the acquired MDR in cancer cell lines.[28,29]The cellular uptake assay further demonstrated that free drugs with a hydrophobic nature were hardly taken up by cells. However, HM showed an elevated uptake in A549/Dox cells. The competitive uptake assay strongly suggested that the surface-anchored HA was involved in the variations of cellular uptake between different formulations, which suggested that HA modification might be able to guide the DDS to the CD44 receptor overexpressed cells with high affinity for the same molecule.[30]

The *in vivo* targeting assay in the current study clearly demonstrated that the tumour targeting nature of HA could guide the HM to accumulate in the *in vivo* tumour tissue.[31,32] Moreover, the *in vivo* antitumour assay further confirmed the enhanced anticancer benefits of Dox and Que in the current study.

In conclusion, this current study manufactured a DDS capable of delivering Dox and Que in the same platform (HM/Dox/Que nanoparticles) for the synergistic chemotherapy of lung carcinoma *in vitro* and *in vivo*. The results demonstrated that HM/Dox/Que was a stable DDS with high biocompatibility. Moreover, HM/Dox/Que was pH responsive with preferential tumour targeting. Most importantly, the *in vitro* and *in vivo* anticancer benefits of HM/Dox/Que were both greatly elevated as compared with the mono-drug delivery systems, which could reverse the MDR, increase the rate of apoptosis and trigger cell arrest of treated cancer cells.

Declaration of conflicting interest

The authors declare that there are no conflicts of interest.

Funding

We acknowledge financial support from the 2018 Medical and Health Research Projects in Zhejiang Province (no. 2018KY837).

ORCID iD

Guobiao Yang https://orcid.org/0000-0003-1605-2844

References

1. Wang C, Wang Z, Zhao X, et al. DOX loaded aggregation-induced emission active polymeric nanoparticles as a fluorescence resonance energy transfer traceable drug delivery system for self-indicating cancer therapy. *Acta Biomater* 2019; 85: 218–228.
2. Meng Z, Zhou X, Xu J, et al. Light-triggered in situ gelation to enable robust photodynamic-immunotherapy by repeated stimulations. *Adv Mater* 2019; 31: e1900927.
3. Xiong H, Ni J, Jiang Z, et al. Intracellular self-disassemble polysaccharide nanoassembly for multi-factors tumor drug resistance

modulation of doxorubicin. *Biomater Sci* 2018; 6: 2527–2540.
4. Li SZ, Zhao Q, Wang B, et al. Quercetin reversed MDR in breast cancer cells through down-regulating P-gp expression and eliminating cancer stem cells mediated by YB-1 nuclear translocation. *Phytother Res* 2018; 32: 1530–1536.
5. Zou Z, Zou R, Zong D, et al. miR-495 sensitizes MDR cancer cells to the combination of doxorubicin and taxol by inhibiting MDR1 expression. *J Cell Mol Med* 2017; 21: 1929–1943.
6. Zhang X, Li Y, Wei M, et al. Cetuximab-modified silica nanoparticle loaded with ICG for tumor-targeted combinational therapy of breast cancer. *Drug Deliv* 2019; 26: 129–136.
7. Meng N, Zhou ZW and Chen QY. c(RGDyK) Peptide-Conjugated Pluronic Micelle for the Effective Delivery of Epirubicin in Glioblastoma: Combination of Radiotherapy and Chemotherapy. *J Biomater Tiss Eng* 2018; 8: 1551–1557.
8. Zhao X, Tang D, Yang T, et al. Facile preparation of biocompatible nanostructured lipid carrier with ultra-small size as a tumor-penetration delivery system. *Colloids Surf B Biointerfaces* 2018; 170: 355–363.
9. Xiong H, Du S, Zhang P, et al. Primary tumor and pre-metastatic niches co-targeting "peptides-lego" hybrid hydroxyapatite nanoparticles for metastatic breast cancer treatment. *Biomater Sci* 2018; 6: 2591–2604.
10. Li M, Luo Z and Zhao Y. Self-assembled hybrid nanostructures: versatile multifunctional nanoplatforms for cancer diagnosis and therapy. *Chem Mater* 2018; 30: 25–53.
11. Wang C, Han M, Liu X, et al. Mitoxantrone-preloaded water-responsive phospholipid-amorphous calcium carbonate hybrid nanoparticles for targeted and effective cancer therapy. *Int J Nanomedicine* 2019; 14: 1503–1517.
12. Wang C, Liu X, Chen S, et al. Facile preparation of phospholipid-amorphous calcium carbonate hybrid nanoparticles: toward controllable burst drug release and enhanced tumor penetration. *Chem Commun (Camb)* 2018; 54: 13080–13083.
13. Tang D, Zhao X, Yang T, et al. Paclitaxel prodrug based mixed micelles for tumor-targeted chemotherapy. *RSC Adv* 2018; 8: 380–389.
14. Lin W and Lee WC. Polysaccharide-modified nanoparticles with intelligent CD44 receptor targeting ability for gene delivery. *Int J Nanomedicine* 2018; 13: 3989–4002.
15. Akhter MH, Rizwanullah M, Ahmad J, et al. Nanocarriers in advanced drug targeting: setting novel paradigm in cancer therapeutics. *Artif Cells Nanomed Biotechnol* 2018; 46: 873–884.
16. Akhter MH and Amin S. An investigative approach to treatment modalities for squamous cell carcinoma of skin. *Curr Drug Deliv* 2017; 14: 597–612.
17. Tang QS, Chen DZ, Xue WQ, et al. Preparation and biodistribution of 188Re-labeled folate conjugated human serum albumin magnetic cisplatin nanoparticles (188Re-folate-CDDP/HSA MNPs) in vivo. *Int J Nanomedicine* 2011; 6: 3077–3085.
18. Tu X, Min LF, Chen QO, et al. Study on Using Magnetic Iron Oxide Nanoparticles as HIF-1 alpha shRNA Gene Carrier to Reverse Cisplatin Resistance of A549/CDDP Cell Lines. *Prog Biochem Biophys* 2010; 37: 1090–1100.
19. Bao X, Gao M, Xu H, et al. A novel oleanolic acid-loaded PLGA-TPGS nanoparticle for liver cancer treatment. *Drug Dev Ind Pharm* 2015; 41: 1193–1203.
20. Chen SQ, Wang C, Tao S, et al. Rational Design of Redox-Responsive and P-gp-Inhibitory Lipid Nanoparticles with High Entrapment of Paclitaxel for Tumor Therapy. *Adv Healthc Mater* 2018; 7: e1800485.
21. Man DK, Casettari L, Cespi M, et al. Oleanolic acid loaded PEGylated PLA and PLGA nanoparticles with enhanced cytotoxic activity against cancer cells. *Mol Pharm* 2015; 12: 2112–2125.
22. Shanmugam MK, Dai X, Kumar AP, et al. Oleanolic acid and its synthetic derivatives for the prevention and therapy of cancer: preclinical and clinical evidence. *Cancer Lett* 2014; 346: 206–216.
23. Daglioglu C. Enhancing tumor cell response to multidrug resistance with pH-sensitive

quercetin and doxorubicin conjugated multifunctional nanoparticles. *Colloids Surf B Biointerfaces* 2017; 156: 175–185.
24. Ramasamy T, Ruttala HB, Chitrapriya N, et al. Engineering of cell microenvironment-responsive polypeptide nanovehicle co-encapsulating a synergistic combination of small molecules for effective chemotherapy in solid tumors. *Acta Biomater* 2017; 48: 131–143.
25. Lv L, Liu C, Chen C, et al. Quercetin and doxorubicin co-encapsulated biotin receptor-targeting nanoparticles for minimizing drug resistance in breast cancer. *Oncotarget* 2016; 7: 32184–32199.
26. Tan LW, Ma BY, Zhao Q, et al. Toxicity evaluation and anti-tumor study of docetaxel loaded mPEG-polyester micelles for breast cancer therapy. *J Biomed Nanotechnol* 2017; 13: 393–408.
27. Wang C, Yu F, Liu X, et al. Cancer-specific therapy by artificial modulation of intracellular calcium concentration. *Adv Healthc Mater* 2019; 8: e1900501.
28. Wen L, Liang C, Chen E, et al. Regulation of multi-drug resistance in hepatocellular carcinoma cells is TRPC6/calcium dependent. *Sci Rep* 2016; 6: 23269.
29. Sun S, Gebauer D and Cölfen H. A solvothermal method for synthesizing monolayer protected amorphous calcium carbonate clusters. *Chem Commun (Camb)* 2016; 52: 7036–7038.
30. Wang C, Chen S, Wang Y, et al. Lipase-triggered water-responsive "Pandora's Box" for cancer therapy: toward induced neighboring effect and enhanced drug penetration. *Adv Mater* 2018; 30: e1706407.
31. Hu Z and Deng Y. Superhydrophobic surface fabricated from fatty acid-modified precipitated calcium carbonate. *Ind Eng Chem Res* 2010; 49: 5625–5630.
32. Semalty A, Semalty M, Rawat BS, et al. Pharmacosomes: the lipid-based new drug delivery system. *Expert Opin Drug Deliv* 2009; 6: 599–612.